Enhancement of the Concrete-PCM Interfacial Bonding Strength using Silica Fume

Mahmudul Hasan MIZAN[1], UEDA Tamon[2*], MATSUMOTO Koji[1]

[1] Hokkaido University, Sapporo, Hokkaido 060-8628, Japan
[2] Shenzhen University, Shenzhen, Guangdong 518060, China

Abstract: Recently, the polymer cement mortar (PCM) overlaying method has gained popularity as a repair/retrofitting technique. The debonding issue at the interface hinders the worldwide application of this strengthening method. Accompanying the occurrence of debonding at the interface, the strengthening effect of the PCM is lost, causing a sudden decrease in the load-carrying capacity. To prevent premature debonding, this study aims to enhance the concrete-PCM interface by using silica fume. The bi-surface shear test was selected as the test method, and three levels of surface roughness (highest level with sandblasting, medium and lowest levels with steel wire brushing) and two different concrete compressive strengths (low strength type (LS) with 16.73 MPa and normal strength type (NS) with 29.59 MPa) were given as experimental parameters. When the surface is roughened by sandblasting, the specimens with 5% silica PCM increase the interfacial strength compared to that of the normal PCM cases by approximately 36.84% and 35.05% for the “LS” and “NS” types of concrete, respectively. The percentage increase is even higher when the surface is roughened by steel wire brushing (high and low), with an increase of approximately 135.35% and 181.12%, respectively. This fact indicates that silica fume inclusions can enhance the chemical bonding at the concrete-PCM interface. The mixing of silica fume in PCM and a higher surface roughness level shifts the pure interface failure (I) mode closer to the concrete cohesion (C) failure mode for “LS” type concrete and to the composite fracture mode (I-P) for “NS” type concrete. Conclusively, it is confirmed that mixing silica fume into PCM strengthened the interface bonding strength.

Keywords: Polymer cement mortar, overlaying method, premature debonding failure, interfacial strength, silica fume

1. Introduction

The twentieth century saw a dramatic increase in large construction projects made from reinforced concrete (RC) around the globe. These structures are at risk of deterioration due to their exposure to various severe environments. Previously, serious accidents occurred that not only caused substantial monetary damage but also damage to livelihoods, including human lives. Instead of replacing these deteriorating structures, repairing and strengthening them is a better solution from both economic and environmental viewpoints. Therefore, the important task in civil engineering is to determine an efficient method for restoring deteriorated concrete construction and to simultaneously ensure the highest level of safe operation.

Numerous experimental and analytical research works are being carried out around the globe and have been done in the past to propose suitable strengthening techniques to achieve the full serviceability of deteriorated structures. Most procedures involved in the rehabilitation/strengthening process require special materials, techniques, and knowledge, making rehabilitation a complex task. Traditional materials and methods are also used as a means to reduce the cost of the intervention. Over recent decades, strengthening techniques such as external post-tensioning [1], FRP jacketing [2], steel plate bonding [3,4], continuous fibre sheet bonding [5], and cement matrix-based methods [6,7] have been proposed based on practical experience and scientific research and are currently in use after exhaustive studies. However, some drawbacks hinder the worldwide application of these strengthening techniques, such as debonding issues at the interface of the concrete and repair material, the cost of the repair materials, difficulties in applying on humid surfaces, susceptibility to UV radiation, poor fire resistance, and chemical damage. To overcome some of these obstacles, alternative research has been carried out by applying polyparaphenylene benzobisoxazole-fibre reinforced cementitious mortar [8] and polymer cement mortar (PCM) [9].

Recently, the PCM overlaying method has gained popularity worldwide as a repair/retrofitting material due to its higher flexural strength and ductility, higher adhesive strength with substrate concrete compared to normal cement mortars, and lower permeability [10]. In this method, cementitious material such as PCM is sprayed/trowelled onto the surface of concrete structures to increase the cross-sectional area of the structures and improve construction durability. This method

relies on the adhesive force of the PCM itself. Among all cementitious materials, polymer-modified cement mortar provides good adhesion at the interface because polymer films surround the hydration products and aggregates. The coalescence of polymer particles fills all the pores, reduces the porosity, and increases the adhesive strength [11,12].

The PCM overlaying method often upgrades the flexural capacity and stiffness of strengthened RC structures. Based on previous experimental studies [13,14,15], it has been established that the bond between the substrate concrete and PCM presents a weak link in the composite structure, and premature debonding failure of the overlay was found to be one of the major failure modes of PCM-strengthened RC beams. In the PCM application, the provision of a good bond between the substrate concrete and overlay is an important requirement for restoring the monolithic character. The bond behavior at the concrete-PCM interface particularly influences the structural performance. The premature debonding failure depicts that the retrofitted structure fails at a lower load than the designated load carrying capacity and cannot achieve full serviceability. In light of the weak bond at the concrete-PCM interface, how this interface can be more effectively improved to prevent the premature debonding failure mode is now a matter of great concern. In general, the success of the intervention relies on the interface capacity to transmit stresses and ensure monolithic behavior. Therefore, the shear stress and strength along the interface have been the object of studies by numerous authors and continuously been revised over the years [16]. Concerning the abovementioned issue, this study aims to increase the interface bonding between existing concrete and PCM using silica fume and surface penetrant with a provision to prevent brittle debonding failure in the PCM overlay strengthening technique. In the past, almost no studies investigate the chemical bonding mechanism of substrate concrete and repairing materials to increase the interfacial bonding, while it is known that free alkali after the hydration of cement reacts with the silica compound of silica fume to produce C-S-H, which strongly affects the bonding strength.

The bonding between the substrate concrete and repair material is also highly influenced by various factors, as reported in previous investigations, such as the surface roughness of the substrate concrete [17,18], moisture condition of the concrete [19], and substrate concrete compressive strength [20]. Environmental conditions such as temperature also affect the interfacial bond properties. An

average reduction in the interfacial shear strength of approximately 18% and 35% were reported by Miura [10] for specimens exposed to 40°C and 60°C, respectively, compared to 20°C, while the surface roughness was introduced by sandblasting. Although different factors have an impact on the interfacial bonding strength, in this study, the effect of surface preparation techniques (three levels of surface roughness: highest level with sandblasting, medium and lowest levels with steel wire brushing) and two different concrete compressive strengths (low strength type (LS) with 16.73 MPa and normal strength type (NS) with 29.59 MPa) were considered as the experimental parameters for the concrete-PCM bond performance as a priority basis.

2. Bonding mechanism

The mechanisms of the bond strength at the interface between the new overlay layer and old substrate concrete are described under 'bond-adhesive' and 'bond-cohesive' mechanisms. The 'adhesive' mechanism is related to the embedding action between the reactive matrix materials of the new material and the old substrate concrete, and the 'cohesive' mechanism is linked to the 'overlay transition zone' of the new material. These two mechanisms are closely associated, and if the bond-adhesive strength is not developed, the interface cohesive mechanism will not be effective. Thus, good adhesion at the interface is required for a successful repair. In general, concrete and PCM are connected at the interface by micro filler and the anchoring effect of the PCM. The PCM overlaying interface is mainly bonded by mechanical bonding, as shown in Fig. 1 (without chemical bonding), despite concrete and PCM parts relying on chemical bonding.

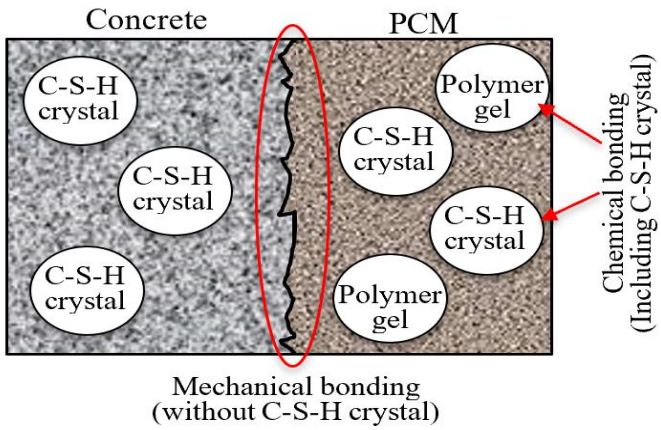

Fig. 1 Schematic diagram of bonding of the PCM overlaying interface

It is thought that the existence of C-S-H crystals affects the bonding strength. Therefore, if C-S-H crystals could also be made to improve the interface between the concrete and PCM, it is expected that the interfacial bond strength will increase to prevent debonding failure. Thus, this study aims to increase the interface bonding strength by using silica fume.

The higher surface area, very high amorphous silicon dioxide content (approximately 90%), and extreme fineness of silica fume make it highly reactive [21]. Additionally, the presence of silica fume accelerates the hydration of the main constituents of cement, i.e., A-lite (C_3S), B-lite (C_2S), and ferrite (C_4AF) [22, 23]. After the hydration of cement, the free alkali, in the form of calcium hydroxide [$Ca(OH)_2$], reacts with the silica compound of silica fume under the water supply condition to form an additional binder material called calcium silicate (C-S-H) hydrate [24], which strongly affects the bonding strength. Additionally, reactive-type sodium silicate surface penetrant is used to re-react the cured concrete to cause cured concrete hydration, as hydration of both cured concrete and PCM is required to form a chemical bond between these two materials. However, cured substrate concrete cannot easily undergo chemical reactions. With this aim, in our previous study [25], 2.5% and 5% silica fume of the PCM mass was used with and without surface penetrant. It was found that the application of surface penetrant to an interface can decrease the interface strength if the application time is inappropriate, and it was suggested that the surface penetrant should be applied approximately 8 hours before the application of PCM to give enough time for the chemical reaction to take place between the surface penetrant and substrate concrete. Although a slight decrease in the interfacial shear strength in the case of 2.5% silica PCM compared to the normal PCM case was observed for the experimental results, an improvement in the interfacial shear strength of approximately 26% was observed in the 5% silica PCM case compared to the normal PCM case.

3. Outline of the test

3.1 Materials and mix proportion

In this study, four types of materials were used: concrete, PCM, silica fume, and surface penetrant. Their mix proportions are discussed in the following sections.

3.1.1 Substrate concrete

Two kinds of concrete with mix ratios, as shown in Table 1, were cast in the laboratory for this

research. Concrete with a higher W/C was termed as “LS” type concrete, and concrete with a lower W/C was referred to as “NS” type concrete. Concrete was cast with commercially manufactured ordinary Portland cement (OPC) in the case of “LS” type concrete and with high early strength cement in the case of “NS” type concrete. Crushed stone with a maximum size of 19 mm for the coarse aggregates and river sand as the fine aggregates were used for both types of concrete.

Table 1 Mix proportions of concrete

Type of Concrete	W/C (%)	Water (L)	Amount(kg/m^3)		
			Cement	Sand	Aggregate
LS	60.0	160	266.67	816.75	1067.4
NS	40.0	160	400.0	788.0	1128.2

3.1.2 Polymer cement mortar (PCM)

As an overlaying material, PCM was used in this experimental work. Commercially available PCM supplied by Denka company was used, with polyacrylic ester (PAE) polymer. The supplied PCM was mixed with the desired amount of water at the time of application, and the mixture became ready to be used. In this study, PCM was cast in the laboratory by mixing 1 bag of 12.5 kg of PCM with 1.9 kg of water (Denka company’s recommendation) before applying PCM over the concrete surface.

3.1.3 Silica fume

As a means to increase the interfacial bonding strength between the concrete and PCM, silica fume was used in this experimental work. In general, the use of a substantial amount of silica fume causes a lack of water because it consumes a substantial amount of water due to its small particle size. Therefore, a large amount of silica fume may cause material stagnation, whereas a very small amount of silica fume hinders the formation of the required C-S-H crystals at the interface, which does not satisfy the interface strengthening requirement [25,26]. In this study, a silica fume content of 5% of the PCM mass was mixed with premixed PCM to prepare silica fume PCM. Silica fume was mixed into PCM powder immediately before mixing with water.

3.1.4 Surface penetrant

As a second improving material of the interfacial bonding strength between the concrete and PCM, a surface penetrant (SP) supplied by the Fuji Chemical Co., Ltd. was used in this test. A reactive

type of (silicate-based) surface penetrant was utilized in the test. The main component of the surface penetrant was “sodium silicate”. The surface penetrant was applied to the substrate concrete surface 8 hours before the application of the PCM layer, as shown in Fig. 2. A pipette was used for the uniform application of the surface penetrant over the entire concrete surface. According to the application guidelines for the surface penetrant by Fuji Chemical Co., Ltd. [27], the surface of the concrete should be maintained with a 6 to 7% moisture level measured with a KTT moisture meter before the application of the surface penetrant. Surface penetrant was applied twice with a time interval of 60 minutes, and the amount was maintained at 0.15 l/m^2 for each of the 1st and 2nd applications. Although the moisture content of the substrate concrete was not measured, attention was paid to the wet condition of the surface of the substrate concrete before application of the surface penetrant and casting of the PCM layer. For the situation where some portion of the surface penetrant remained over the concrete surface, it was wiped before the application of the PCM layer.

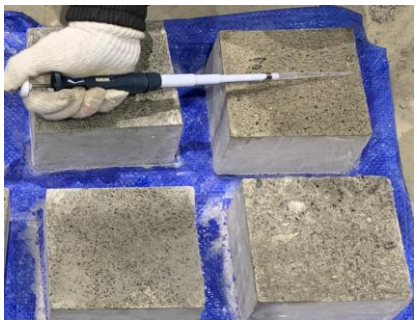

Fig. 2 Application of the surface penetrant over the concrete surface

3.2 Specimen preparation

3.2.1 Bulk specimens

Cubic specimens with a size of 150 x 150 x 150 mm and 100 x 100 x 100 mm for measuring the shear strength and cylindrical specimens with a size of 100 x 200 mm and 50 x 100 mm for measuring the compressive strength were cast for concrete and PCM, respectively. Following the previous study [28, 29], different sizes of bulk concrete and PCM specimens were selected to reduce the material use of PCM. After casting, the molds were covered with a polythene sheet to avoid the evaporation of moisture. All the specimens were de-molded after 24 hours. All the concrete specimens were cured for 28 days in wet conditions, whereas the specimens containing PCM were cured for 7 days (wet curing) to help in the hydration process and 21 days (dry curing) to form polymer films that could fill the

voids and strengthen the PCM [30].

3.2.2 Composite specimens

3.2.2.1 Surface preparation

For the preparation of composite specimens, concrete cubical specimens with a size of 150 x 150 x 100 mm were cast first. One surface of the specimen with a size of 150 x 150 mm was roughened by steel wire brushing (WB) and sandblasting (SB) methods for better interlocking of the overlay layer to the substrate layer, as these methods generate fewer micro-cracks in the substrate layer [16]. Two types of roughness levels were prepared by the WB technique and categorized as low (L) and high (H). Eight hours after the concrete was cast, steel wire brushing was performed in the laboratory by the author. The types of cement used in the specimen preparation results in the difference in the surface roughness level. The specimens cast with high early strength Portland cement resulted in a lower roughness level with no exposure of coarse aggregate, as shown in Fig. 3(a), whereas the specimens cast with normal strength Portland cement resulted in a higher roughness level with some exposed aggregates, as shown in Fig. 3(b), thus named WB(L) and WB(H), respectively. On the other hand, sandblasting was performed after 14 days of curing of the concrete, and it was observed that the types of cement used in the specimen preparation did not result in different surface roughness levels, as shown in Fig. 3(c). Following the outcomes of the trial test (in WB cases) by the author and previous group research in our team [10, 25] (in SB cases), paying good attention, it is possible to get similar roughness level of the three specimens used in each group by visual inspection. Also, the considered roughness level as shown in Fig 3(a-c) can be easily identified with visual inspection with minimal scattered roughness value. Thus, qualitative assessment based on the visual inspection method was used to define the roughness level in this study rather than the quantitative analysis that widely used by many researchers.

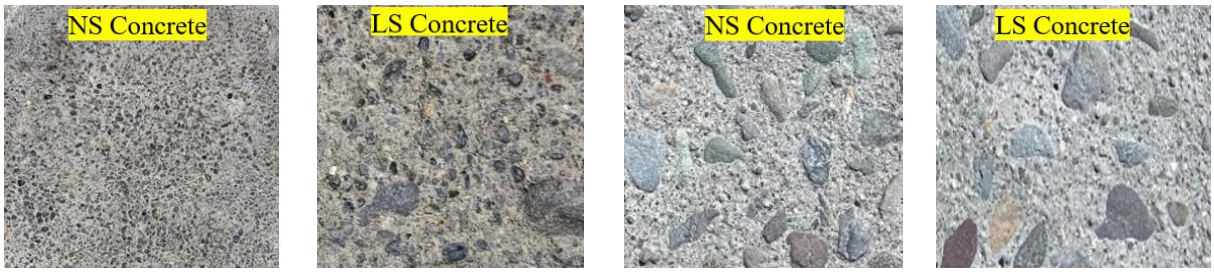

(a) WB(L) (b) WB(H) (c) Sandblasting (SB)

Fig. 3 Treated substrate concrete surface in this test

3.2.2.2 Preparation of the composite specimen

Concrete specimens with a size of 150 x 150 x 100 mm were put into the mold, and the roughened surface was kept facing up in the mold. Before casting the PCM, the top surface of the substrate concrete specimens was cleaned with high air pressure to remove any dust as well as to create microporosity which helps in good adhesion. After that water was sprayed at the top concrete surface following the Guidelines on Design and Application Methods of Silicate-based Surface Penetrant used for Concrete Structure [27] and free water on the rough surface was removed with a towel just before casting the PCM to provide a saturated concrete substrate with a dry surface for adequate bonding [31]. Though moisture content of the substrate concrete was not measured quantitively, good attention was paid to the wet condition of the surface of substrate concrete before casting PCM. Once water stagnation had disappeared, PCM was trowelled over the treated surface of the concrete. The PCM was trowelled in two layers (approximately 25 mm in each layer) with a time interval of 180 minutes, and the mold was filled to produce the specimens of a 150 mm cube, which meant that the cast volume of the PCM was 150 x 150 x 50 mm, as shown in Fig. 4.

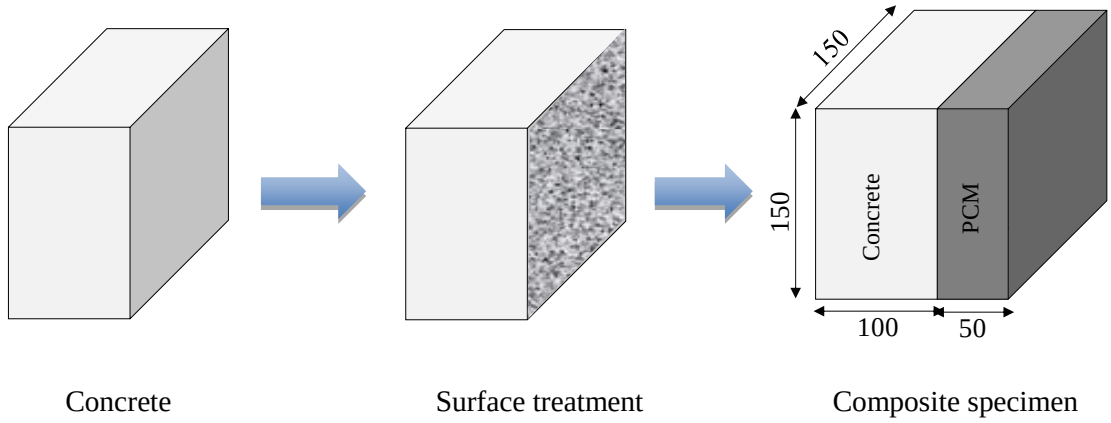

Fig. 4 Procedure of composite specimen preparation for the bi-surface shear test (unit: mm)

The concrete in the composite specimens had already been cured and was in the hardened state, but the PCM was in the fresh state. Thus, composite specimens were cured following the curing process of PCM containing specimens described in Section 3.2.1. The total number of composite

specimens cast is shown in Table 2.

Table 2 Number of composite specimens for the interfacial shear test

Specimen types		Surface roughness preparation		
		Steel wire brushing (Low)	Steel wire brushing (High)	Sandblasting
Composite Specimens	A+C	--	3	3
	A+D	--	3	3
	B+C	3	--	3
	B+D	3	--	3
	A+D with SP	--	3	3
	B+D with SP	3	--	3

Note: A & B denote “LS” and “NS” types of concrete, and C & D denote normal and 5% silica PCM.

3.3 Testing procedure

3.3.1 Bulk specimens

The compressive strengths of both materials, concrete, and PCM, were measured using the standard test method as per ASTM C39 [32]. Compressive testing was performed using a universal testing machine (UTM) available in the laboratory. The average compressive strength of three specimens was recorded as the compressive strength under particular conditions. The shear strength was evaluated by using the bi-surface shear strength test, which was explained in detail by Momayez et al. [33]. The geometry and types of specimens tested for the evaluation of the bi-surface shear strength are shown in Fig. 5(a-b) for concrete and PCM, respectively.

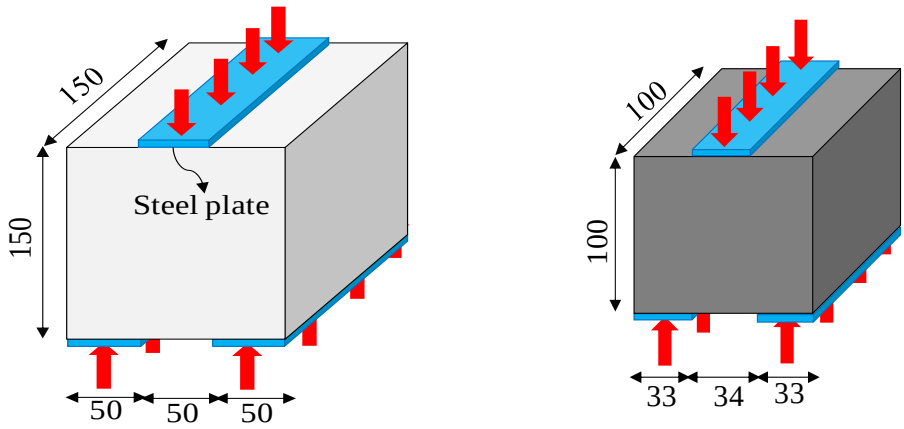

(a) Bulk concrete (b) Bulk PCM

Fig. 5 Schematic diagram of the shear test of the bulk specimen with the loading condition (unit: mm)

Three specimens were tested for each specimen type, and the average shear strength of the three specimens was recorded as the shear strength under particular conditions. The shear strength was evaluated by using the following equation.

$$\tau_v = \frac{P_u}{2A} \tag{4}$$

where τ_v = the shear bond strength (MPa), P_u = the ultimate load (N) and A = the area of the connected interface (mm^2).

3.3.2 Interfacial shear strength of the composite specimens

The interfacial shear strength is one of the major interface properties that need to be carefully investigated. The measurement of the "pure" shear strength has always been a challenge for researchers, as it is a very difficult condition to achieve in reality. Many previous methods have been proposed to quantify the interfacial shear strength [33,34]. Single or double shear tests have been widely used and developed to evaluate the interface shear strength due to their simple loading method, but it has a disadvantage in the possibility to cause not adhesive failure but local compressive failure at the edge of loading plate or bending crack [35]. The slant shear test that evaluated under a combination of compression/tension and shear action at the interface has also been investigated by some researchers and has been developed as a design standard such as ASTM C 882 [36]. The presence of a compression force in the slant shear test leads to higher bonding strength than that in the pure shear stress condition due to the increase in friction. Meanwhile, the test method is greatly

influenced by the difference between the stiffness of substrate concrete and repair material, the geometry of the test such as size and axis at the shear plane [34]. Some researchers have used their developed testing method for the pure interfacial shear strength measurement, but these methods were not widely accepted due to their complex test setups. Each of these tests has been reported to have some advantages and disadvantages compared with one another. Momayez et al. [33] proposed a new direct shear test named bi-surface shear strength test that does not require any special form and can be fabricated easily as well as gives this method gives less variation in the results. Thus, this method is widely used for the evaluation of the interfacial shear strength. Consequently, considering the fact of a large number of specimens with different roughness levels and to ease the complexity in specimen preparation, the bi-surface shear test was adopted to measure interface shear strength in this study. The scheme of the test method used for the measurement of the interfacial shear strength of the composite is shown in Fig. 6. The interfacial shear strength was evaluated by using Equation 4, and the average strength of the three specimens was recorded as the interfacial shear strength under particular conditions.

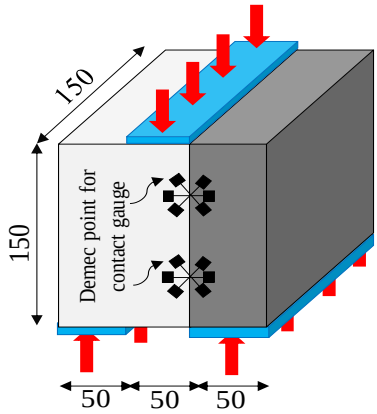

Fig. 6 Schematic diagram for the interfacial shear strength of the composite specimen (unit: mm)

3.4 Interfacial slip measurement

Few studies have been found in the literature on the interface behavior of the concrete and repair material, especially with slip or opening information at the interface. In a previous study [10], a π gauge was used for the measurement of the interfacial slip between the concrete and PCM. In this study, demec points were used, as shown in Fig. 6, at distances of 50 mm and 100 mm from the top edge of the specimens for the measurements of interfacial slip at that particular position. Inclined

demec points were attached in two directions at angles of 45° and 135° with the horizontal direction. The demec point reading was taken by the contact gauge at some particular load during the test.

Using these data, the slip was calculated based on the simple assumption. The average of the two calculated slip values was based on two inclined demec points and one horizontal demec point and was considered the slip at that particular point. Furthermore, the average of the two calculated slip values at two positions is considered the slip of that particular specimen. The calculation method of the slip is shown in Fig. 7(a-e). The line BB′ in Fig. 7(c) is oblique, i.e., not purely horizontal or vertical. Therefore, it can assume two cases where point "B" moves purely horizontally (Case-1, in Fig. 7(d)) and point "B" moves purely vertically (case-2, in Fig. 7(e)).

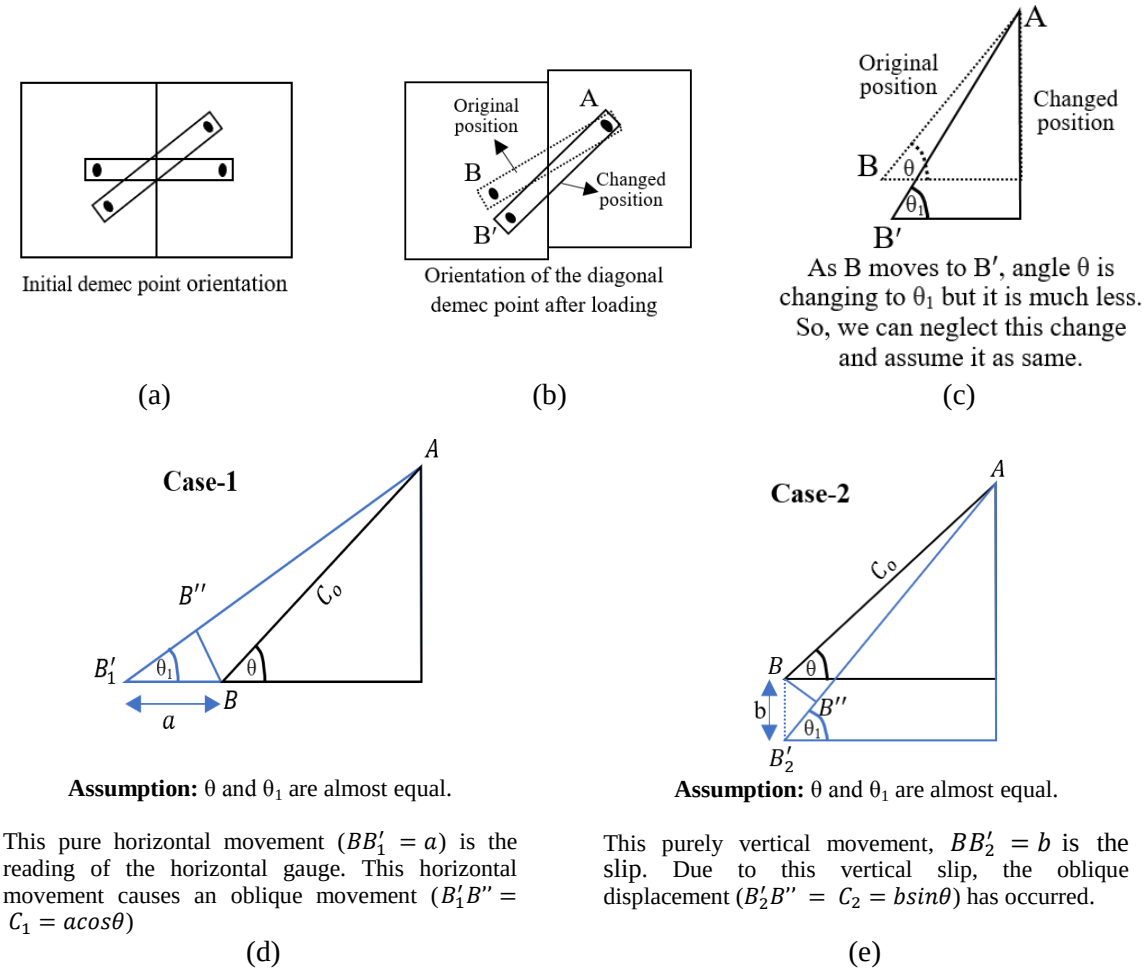

Fig. 7 Calculation procedure of the interfacial slip

In the original situation, $BB' = C$ can be thought of as a combination of case-1 and case-2.

$$C = B_1'B'' + B_2'B'' = acos\theta + bsin\theta$$

$$b(slip) = \frac{(C - acos\theta)}{sin\theta} \quad (5)$$

where a: opening measured by the horizontal gauge, b: slip, C: (= C_1 + C_2) displacement measured by the inclined gauge, C_1 and C_2: decomposed displacement measured by the inclined gauge, C_o: initial reading of the inclined gauge, θ_1: angle at the concerning displacement, and θ: initial angle

4. Test results and discussions

4.1 Bulk specimens

The compressive and shear strengths of both materials, the concrete and PCM, were evaluated for the cylindrical and cubical specimens, where both strengths were expressed as the average of the three specimens. The average strengths along with the standard deviation and coefficient of variance of all the bulk specimens are presented in Table 3.

Table 3 Average compressive and shear strengths of all the tested monolithic specimens

Specimen types	Test type					
	Compressive			Shear		
	Strength (MPa)	SD (MPa)	COV (%)	Strength (MPa)	SD (MPa)	COV (%)
LS concrete (A)	16.73	1.65	9.87	4.53	0.36	7.96
NS concrete (B)	29.59	2.38	8.06	7.82	0.26	3.28
Normal PCM (C)	74.75	0.25	0.34	6.24	0.43	6.88
5% silica PCM (D)	59.06	3.1	5.25	7.23	0.29	3.95

Note: SD - standard deviation, COV - coefficient of variance

4.2 Composite specimens

4.2.1 Interfacial shear strength

Table 4 Interface shear strength (average) of all the tested composite specimens

Overlay parameters	Substrate concrete parameters	Bi-surface Shear Strength		
		Interfacial Strength (MPa)	SD (MPa)	COV (%)
Normal PCM	NSC_SB	3.24	0.38	11.85
	LSC_SB	2.86	0.42	14.71
	NSC_WB(L)	0.63	0.04	7.14
	LSC_WB(H)	1.17	0.08	6.85

5% silica PCM	NSC_SB	4.38	0.46	10.58
	LSC_SB	3.92	0.51	13.03
	NSC_WB(L)	1.77	0.13	7.34
	LSC_WB(H)	2.76	0.12	4.23
5% silica PCM with SP	NSC_SB	1.50	0.13	8.48
	LSC_SB	1.22	0.12	9.87
	NSC_WB(L)	0.38	0.03	7.70
	LSC_WB(H)	0.71	0.02	1.41

Note: NSC-Normal Strength Concrete, LSC- Low Strength Concrete

The interface shear strengths of the composite specimens were evaluated by the bi-surface shear test. The average strengths along with the standard deviation and coefficient of variance of all the composite specimens are presented in Table 4. There were three specimens in each group. The data of the particular specimens were excluded when the difference value between any measured value and the mean value calculated exceeds 20% of the mean value, the median value measured is taken as the mean value. The COV values ranged from 1.41% to 14.71% which are reasonable considering the variability of production of cementitious composites. A large variation in SD and COV value were also observed in interfacial shear strength test in previous studies [25,37,38].

The constituent of the overlay material attached to the substrate concrete influenced the interfacial bonding strength. The inclusion of 5% silica fume of the PCM mass in the overlay material greatly increased the interfacial strength in each substrate concrete compressive strength and surface roughness case. The percentage increases in the interfacial strength for the case of 5% silica PCM compared to the normal PCM cases are presented in Fig. 8. The increasing percentage is very high for the steel wire brushing cases with both the medium and lowest surface roughness levels compared to the sandblasting case that has the highest surface roughness level. This fact indicates that silica fume inclusions can enhance the chemical bonding at the concrete-PCM interface. Therefore, in practical PCM strengthening applications, the inclusion of silica fume in the overlay material is highly suggested if the substrate concrete cannot meet the roughness requirements.

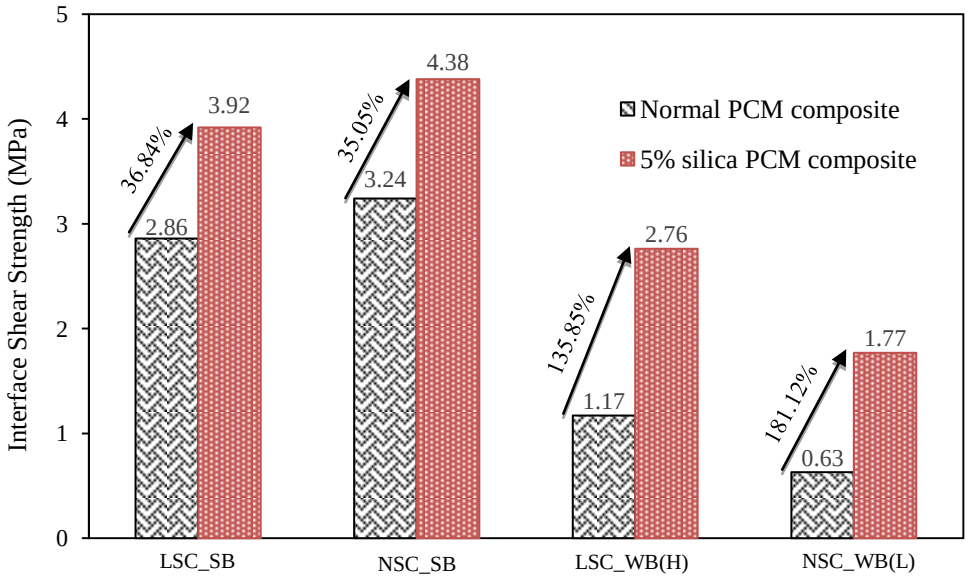

Fig. 8 Increase in the interface shear strength by the inclusion of silica fume in PCM

The composite specimens (5% silica PCM with SP) show less interfacial shear strength compared to normal PCM composites irrespective of the types of concrete or surface roughness level as shown in Fig. 9 which indicates that our initial thought on the possible enhancement of the bond strength by silicate-based surface penetrant was not correct. One of the reasons for the reduction in the interfacial bonding strength is the presence of a white compound in both the concrete and PCM parts in the specimens with the surface penetrant, as shown in Fig. 10(a). In a previous study [25], this white compound was also observed at the interface of the specimens with surface penetrant, and the presence

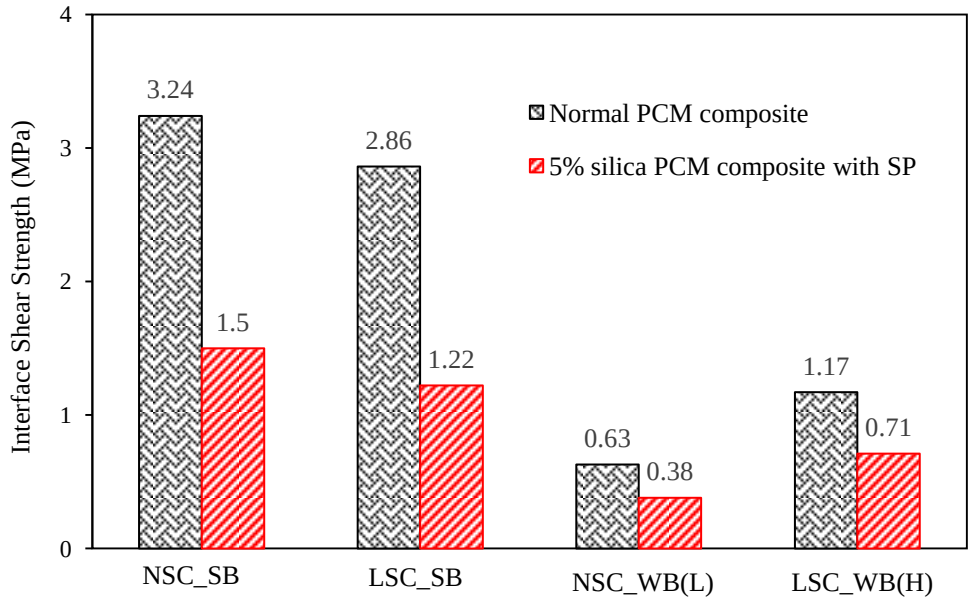

Fig. 9 Decrease in the interface shear strength in %5 silica PCM with SP compared to normal PCM composite

of 44% $CaCO_3$ was found by X-ray diffraction analysis of the white compound, which was higher compared to that of the normal concrete cases (approximately 20%). This white compound cannot be seen in the normal PCM cases or the cases without the surface penetrant, as shown in Fig. 10(b). Another cause for the reduction in the interface shear strength is that the layer of the surface penetrant over the substrate concrete acts as a protective layer. In general, this material is used over the cured concrete surface as a surface modifier to protect the surface from abrasion, water penetration, etc. This protective layer hinders the flow of the water to the cured concrete, which is required for hydration and prevents the small silica fume and PCM particles from filling the gaps among the cement particles of the substrate, resulting in a weak bond between the substrate concrete and overlay layer. In the SP application, it is realized that it is very important to adjust the chemical reaction time of SP and PCM. The intensive chemical reaction time between concrete and SP which depends on the kinds of SP used has not been studied so well. Therefore, more tests on SP application are intending to do in our future research to know the exact surface penetrant reaction time to realize effective interface bonding.

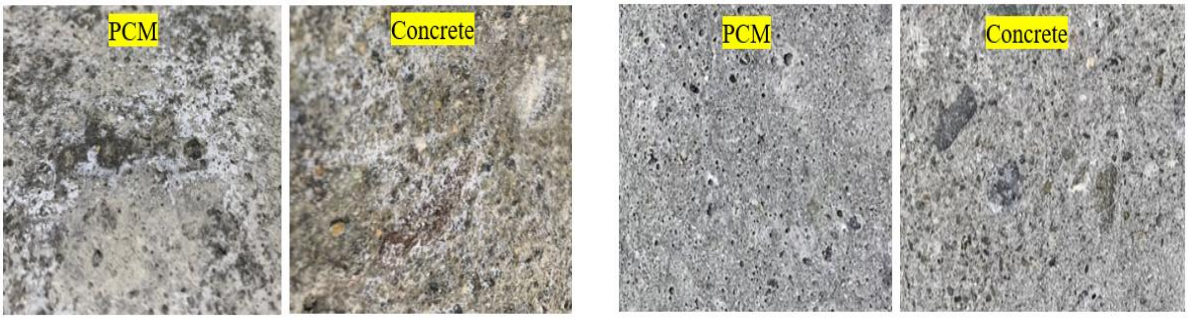

(a) With surface penetrant (b) Without surface penetrant

Fig. 10 White compound in the interface

The results of this study and the previous study [25] with different substrate concrete compressive strengths are compared in Fig. 11(a) when the surface is roughened by sandblasting. The vertical axis indicates the interfacial shear capacity, and the horizontal axis indicates different substrate concrete compressive strengths. An increase in the interfacial shear strength of 13.29% for the normal PCM case and 11.74% for the 5% silica PCM case when the surface was roughened by sandblasting was found in this study for “NS” concrete compared to that of “LS” concrete. In the case of the low substrate concrete compressive strength cases, cracks occur in the concrete earlier and propagate towards the interface, causing failure of the specimens through the interface or with the concrete cohesion fracture mode, subsequently resulting in lower interfacial bonding strength. The increase in the interfacial bonding strength with the increases in the substrate concrete compressive strength was also observed when 5% silica PCM specimens were compared to the normal PCM specimens. The increase percentages were 36.84%, 35.05% and 26.11% for the concrete compressive strengths of 16.73 MPa, 29.59 MPa, and 40.17 MPa, respectively. This indicates that the percentage change in the interfacial strength for the 5% silica PCM compared to that of the normal PCM cases decreased with the increase in the substrate concrete compressive strength.

Fig. 11(b) shows that the interfacial bonding strength decreases with increasing substrate concrete compressive strength. This is because the roughness level is high for the case of the specimens with a lower substrate concrete compressive strength. Conclusively, there is an optimum surface roughness level of the substrate concrete up to which the substrate concrete compressive strength is not effective on the interfacial bonding performance. After the optimum surface level, the interfacial strength

increases with increasing substrate concrete compressive strength.

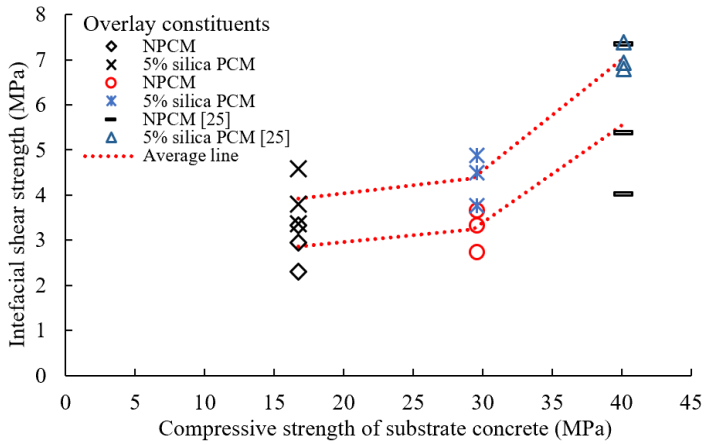

(a) Sandblasting

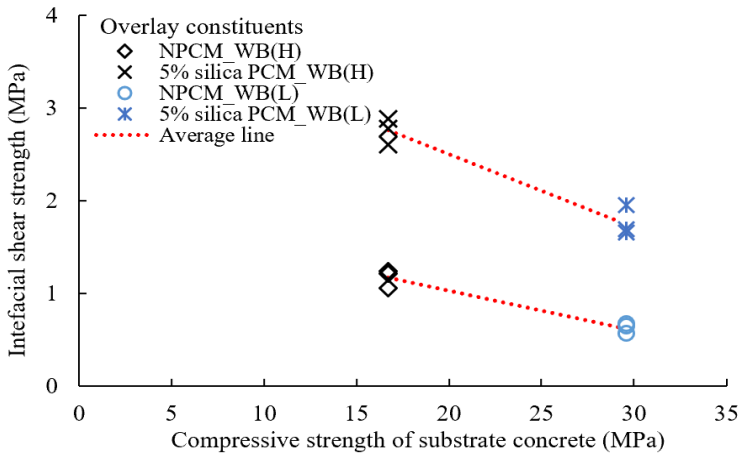

(b) Steel wire brushing

Fig. 11 Effect of the substrate concrete compressive strength on the interfacial bonding at different surface roughness levels.

Many available reports have been discussed [39-42], and it has been concluded that the surface roughness treatment is significantly important for enhancing interface bonding between the substrate concrete and overlay materials. This study also confirmed the positive roughness effect of the substrate concrete on the interfacial bonding performance between the concrete and PCM. From Fig. 12, it is seen that the surface roughness prepared by sandblasting, that has a higher surface roughness level, results in a higher interfacial shear strength than that of the steel wire brushing cases that have a lower surface roughness level for the case of both normal PCM and 5% silica PCM composite specimens. In the case of the normal PCM composite specimens, sandblasted specimens with the highest level of roughness have higher interfacial strengths of approximately 5 times and 2.5 times

compared to the specimens roughened by steel wire brushing (lowest and medium roughness level). Consequently, the surface roughness level greatly influences the interfacial bonding performance both in normal PCM and 5% silica PCM cases.

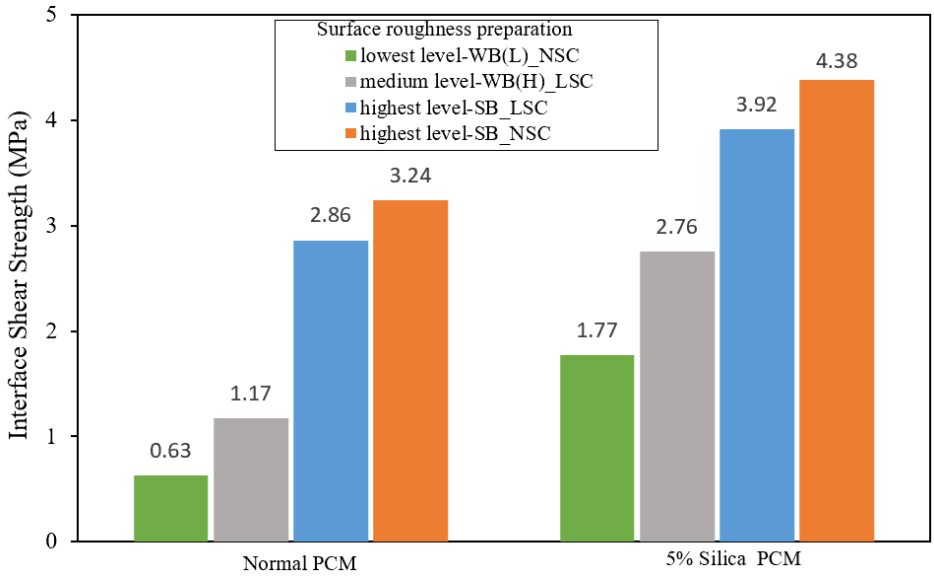

Fig. 12 Variation in the interfacial strength with different surface roughness techniques

4.2.2 Fracture mode of the composite specimens

4.2.2.1 Definition of the fracture mode

The composite specimens are considered a combination of three zones/layers: the PCM cohesion layer, concrete cohesion layer, and interface between the concrete and PCM termed the adhesion layer. The fracture modes are named according to the location of the fracture on the surface of the specimens. In this study, four types of fracture modes were observed. Sometimes, the failure was along with the interface and named the pure interface fracture mode, as shown in Fig. 13(a), with or without tiny cracks in the concrete or PCM. Some failures were categorized as a composite fracture mode. In some cases, especially for low strength substrate concrete, some aggregates were seen attached to the PCM side, as shown in Fig. 13(b), and named the interface-concrete composite fracture mode (I-C). When some PCM is attached to the concrete substrate, as shown in Fig. 13(c), the failure mode was named the interface-PCM composite fracture mode (I-P). Additionally, when the fracture was observed only in the substrate concrete cohesion layer, as shown in Fig. 13(d), the fracture mode was named the concrete cohesion fracture mode (C).

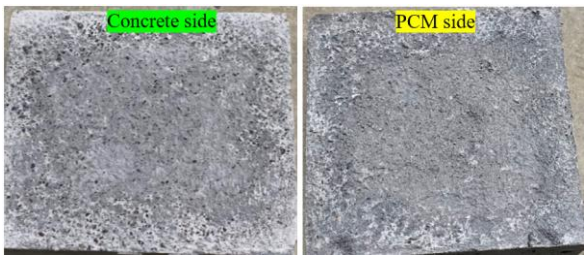

(a) Pure interface fracture (I)

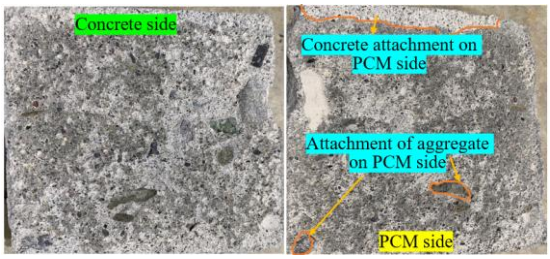

(b) Interface-concrete composite fracture (I-C)

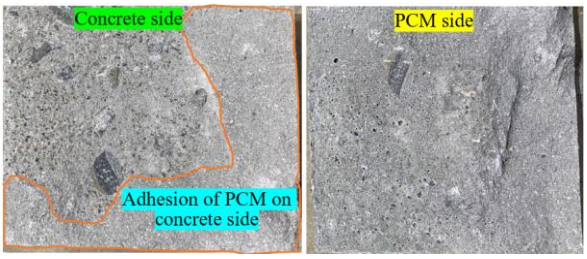

(c) Interface-PCM composite fracture (I-P)

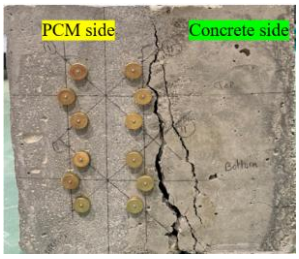

(d) Concrete cohesion fracture (C)

Fig. 13 Sample fracture surface of the composite specimens

4.2.2.2 Observed fracture mode in the composite specimens

In this study, all of the composite specimens with surface penetrant showed pure interface (I) fracture. The fracture modes of the specimens other than the surface penetrant specimens are shown in Fig. 14. The sandblasted specimens showed an increase in the number of specimens that failed at the mixed-mode or concrete cohesion mode in 5% silica PCM cases compared to normal PCM cases. For example, one pure interface fracture mode (I) was observed in the case of specimen LSC_NPCM_SB, but no pure interface fracture mode (I) was observed in the case of specimen LSC_5% silica PCM_SB; rather, the fracture mode shifted to one mixed-mode (I-C) and two concrete cohesion modes (C). It may be considered that concrete cohesion fracture occurred when the interface shear strength was higher than the concrete shear strength. However, for both the normal PCM and 5% silica PCM cases, all the specimens show pure interface fracture mode (I) when the surface is roughened by steel wire brushing (both high and low steel wire brushing cases). Consequently, it can be said that the increase in the surface roughness shifted the failure surface closer to the concrete cohesion (C) side for the case of the low substrate concrete compressive strength and to the mixed-mode (I-P) for the case of the high substrate concrete compressive strength.

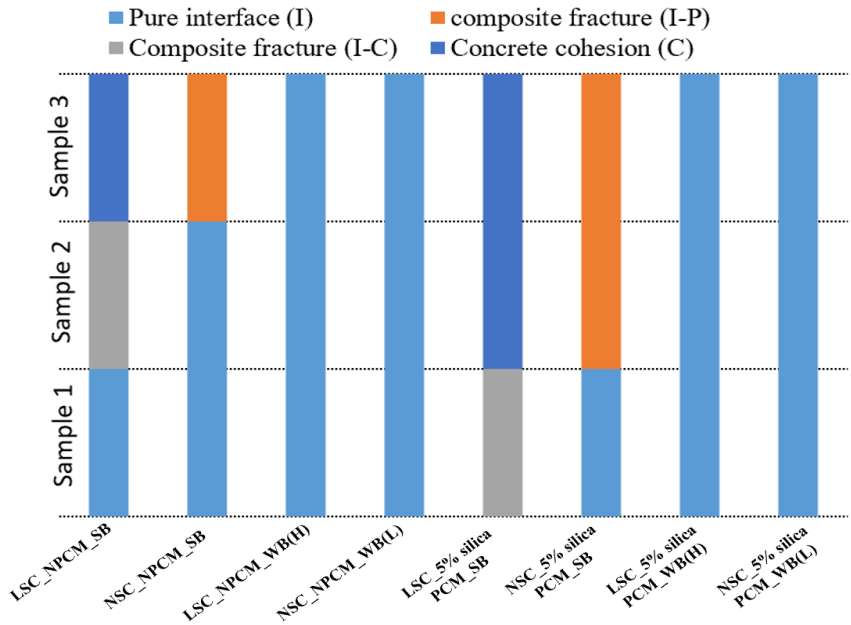

Fig. 14 Fracture mode observed for the composite specimens

4.2.3 Fracture energy

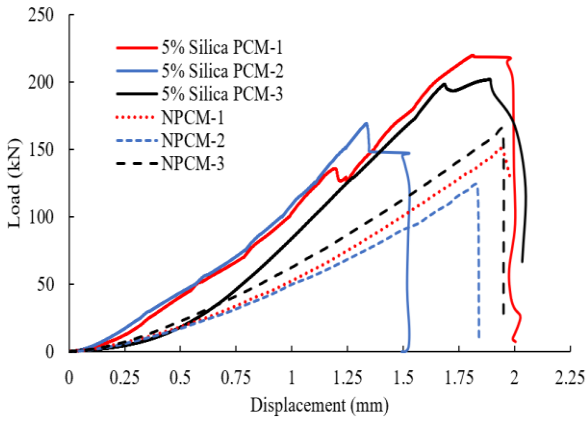

(a) Sandblasting -NS type concrete

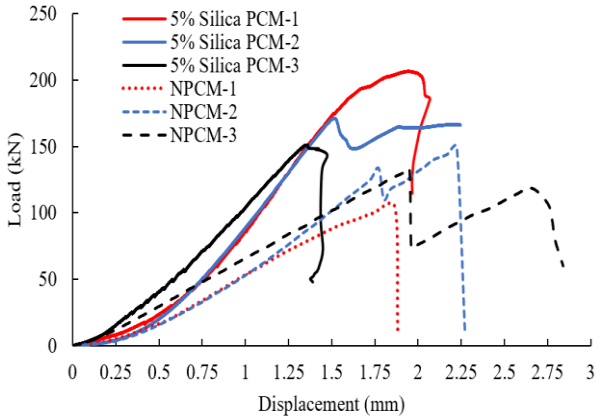

(b) Sandblasting-LS type concrete

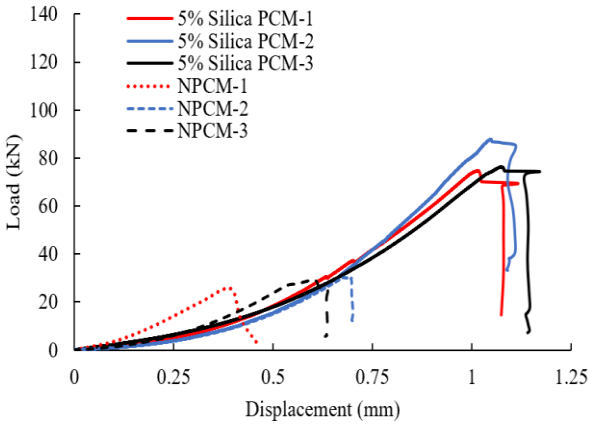

(c) Steel wire brushing (L)- NS type concrete

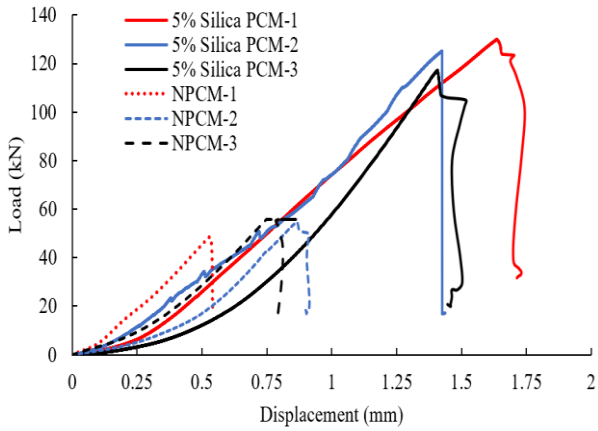

(d) Steel wire brushing (H)-LS type concrete

Fig. 15 Comparison of the load-displacement relationship for normal PCM and 5% silica PCM specimens

Fig. 15(a-d) shows the relationship between the load and displacement where displacement is the vertical deformation measured using LVDT at the mid-position of the specimens during testing that includes bending deformation of the specimen and settlement at the supports. Most of the curves show a sudden drop in the load value due to crack initiation and propagation through the interface representing pure interface or mixed-mode fracture. Only a few curves in Fig. 15(b) show a gradual decrease in the load value, which represents the concrete cohesion fracture mode. The initial stiffness and slope of the curve increase with the inclusion of silica fume on the PCM compared to normal PCM in both the normal and low strength substrate concrete cases, as shown in Fig. 15(a-b), when the surface was roughened by sandblasting. However, for the surface roughness cases with steel wire brushing, the initial stiffness and slope of the curve showed different trends, thus, it is difficult to get any tendency from the graphs (Fig. 15(a-b)) for the normal PCM and 5% silica PCM specimens cases.

The fracture energy was obtained from the area under the load-displacement curve, as shown in Fig. 15(a-d), for the normal PCM and 5% silica PCM cases. The calculated fracture energies of all the tested composite specimens are shown in Table 6.

Table 5 Fracture energy of all the tested composite specimens

Concrete and surface preparation	Specimens No.	Fracture energy (N/mm)		
		Normal PCM	5% silica PCM	5% silica PCM with SP
NSC_SB	1	5.34 (I-P)	9.53 (I-P)	1.11
	2	4.01	5.30	0.52
	3	5.83	8.50 (I-P)	0.89
LSC_SB	1	4.09	9.93 (C)	0.76
	2	6.76 (I-C)	9.50 (C)	0.60
	3	9.39 (C)	5.72 (I-C)	1.23
NSC_WB(L)	1	0.23	1.38	0.19
	2	0.32	1.65	0.21
	3	0.35	1.74	0.18
LSC_WB(H)	1	0.52	4.95	0.80
	2	0.85	3.35	0.47
	3	0.84	3.26	0.32

Note: Letters within the brackets represent the fracture mode of the specimens

The results with the letters within the brackets (I-P), (I-C) or (C) represent the fracture mode of the specimens, whereas the results having no enclosed bracket represent the pure interface fracture mode (I). The concrete cohesion and composite fracture mode correspond to higher fracture energy than that of the pure interface fracture modes. The results also indicate that the specimens that failed by the concrete cohesion fracture mode (C) possess higher fracture energy than the specimens that failed by either the composite (I-P) or (I-C) fracture modes. Besides, the fracture energy of the specimens with 5% silica fume is more than that without the silica fume with few exceptions. Consequently, it can be said that the fracture energy increases with the inclusion of silica fume, which is also affected by the fracture mode of the composite specimens.

4.2.4 Opening and slip of the composite specimens

Demec points were attached in the horizontal and inclined directions, as shown in Fig. 6, and the movement of the concrete and PCM layer along these directions was measured by the contact gauge upon loading to calculate the slip of the specimens. The openings measured by the horizontal demec points of the normal PCM sandblasted specimens are shown in Fig. 16.

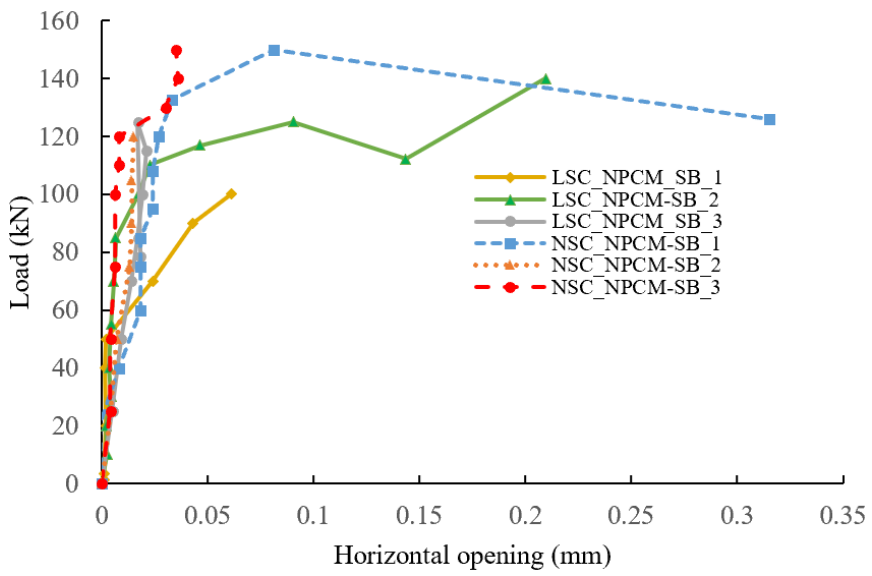

Fig. 16 Load-opening relationship of the NPCM specimens when the surface was roughened by sandblasting

The measured opening value is much less when the specimens failed through the pure interface (I) or concrete cohesion (C) modes compared to the specimens that failed by mixed-mode failure, i.e., both (I-P) and (I-C). In the case of the mixed-mode failure, cracks were seen around the interface

(more precisely within two demec points in the horizontal direction) either in the concrete or PCM part; thus, some openings were measured by contact gauges, as shown in the specimens "LSC_NPCM_SB_2" and "NSC_NPCM_SB_1". However, the crack opening was hardly measured for the case of the other specimens. For the case of the specimens that failed by the concrete cohesion (C) failure mode, cracks were formed in the concrete part outside the range of the demec point; thus, the opening value measured by the contact gauge was very low. Additionally, in the case of pure interface (I) failure, the opening was hardly measured due to sudden brittle failure through the interface without any cracks in either the concrete or PCM part.

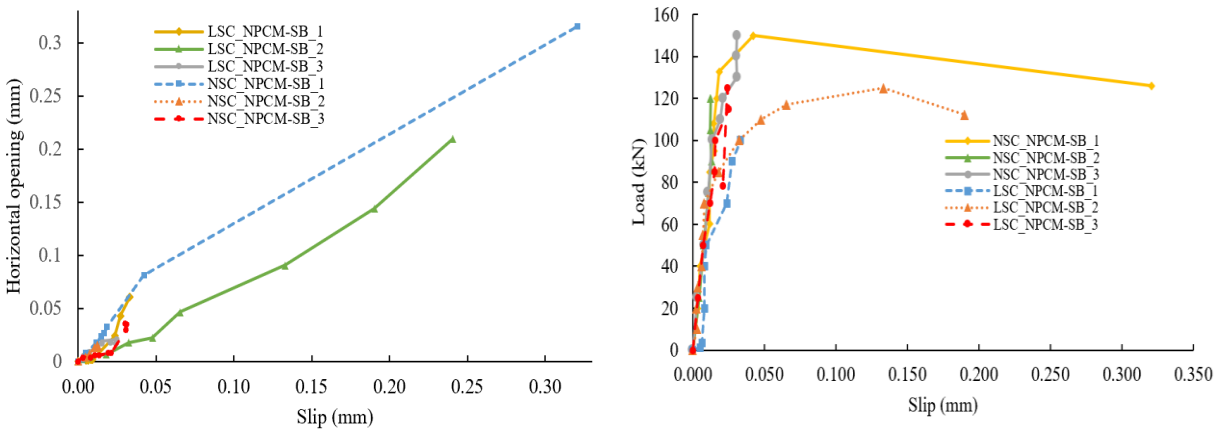

(a) Opening-slip relationship (b) Load-slip relationship

Fig. 17 Relationship of the slip with the opening and load of the NPCM sandblasted specimens

The interfacial slips that includes only the relative displacement in in-place direction of the interfaces were calculated by Equation 5 using the contact gauge data. The relationship between the opening and slip is shown in Fig. 17(a), which indicates that the slip value is directly related to the opening value measured in the horizontal direction, i.e., an increase in the opening values results in a larger interfacial slip. Additionally, the load-slip relationship of the normal PCM sandblasted specimens is shown in Fig. 17(b). The post-peak behavior is hardly present due to sudden brittle adhesion failure that was observed, and the load-slip relationship is found to be almost the same and linear up to the pre-peak region in all cases. Because brittle failure occurred at the interface, it became very difficult to use the contact gauge measurement after it reached the peak load. Additionally, the machine had to continually stop for the use of the contact gauge, which introduced a discontinuity in the measurement, but the continuous measurement is important to obtain the post-peak behavior.

Consequently, demec points with manual measurement techniques are not suitable to measure interfacial slip; instead, automatic continuous measurement techniques using a high-resolution camera and a digital image processor is intending to use in our future research.

4.3 Comparison with a previous study

The comparison between the results of this study and the previous study concerning PCM overlaying at the material level test is shown in Table 6. The observations are summarized as follows:

- The interface shear strength for the case of normal PCM in the study by Rashid *et al.* [43] is higher than that in the study by Miura [10], and this study, though the surface roughness treatment (sandblasting techniques), test type and specimen sizes were the same. This is caused by the higher roughness level of sandblasting. The roughness levels used in this study and in the previous study [43] are shown in Fig. 18.

Fig. 18 Comparison of substrate concrete roughness level by sandblasting in different study

- Many studies in the past discussed the use of bonding agents, for example, primers at the interface to increase the bonding strength. The positive influence of primers was also confirmed in the previous study [43]. However, primers have a negative impact on the environment. The inclusion of the 5% silica fume in this study results in a higher interfacial strength, which is compatible with that of the study by Rashid et al. [43], although no bonding agent was used in this study, and the surface roughness level was lower than that of the previous study.
- The interfacial shear strength in the previous study [25] is much higher than that in the other study mentioned. This difference is mainly caused by the small specimen sizes used and the different test types used. Smaller specimen sizes result in higher interfacial strengths than larger specimen sizes. The same phenomenon was also found in another study [33].

Table 6 Comparison of the parameters and strength between previous studies and this research

	Specimen Size (mm)	Surface preparation	Overlay materials	Interface shear strength (MPa)
Rashid, K. [43]	150x150x150 (Bi-surface shear)	Strong water jetting (Ra as 0.73 mm)	NPCM without primer	3.65
			NPCM with primer	4.55
Miura, S. [10]	150x150x150 (Bi-surface shear)	Sand blasting (Ra as 0.5 mm)	NPCM with primer	3.37
Shibao, H. *et.al* [25]	100x80x70 (Direct single surface shear)	Sand blasting (Ra as 0.48 mm)	NPCM	5.57
			5% Silica PCM	7.03
This study	150x150x150 (Bi-surface shear)	Sand blasting	NPCM	3.24
			5% silica PCM	4.38

Conclusions

The following conclusions can be made from this material level test:

- The interfacial shear strength increases with the increase in the surface roughness level for both the normal PCM and 5% silica PCM cases.
- The substrate concrete compressive strength is not effective in increasing the interfacial bonding strength up to a certain surface roughness level (optimum level) of the substrate concrete. If the roughness level exceeds that of the optimum level, the interfacial bonding strength increases with increasing substrate concrete compressive strength.
- The inclusion of silica fume in the PCM will increase the interfacial bonding strength. Additionally, the mixing of silica fume in the PCM shifts the failure surface closer to the concrete cohesion (C) side for the case of the low substrate concrete compressive strength and to the composite fracture mode (I-P) for the case of the high substrate concrete compressive strength if the surface roughness level is high. However, the surface roughness prepared by steel wire brushing that has a lower surface roughness level result in the pure interfacial fracture mode (I) for both the normal PCM and 5% silica PCM cases.
- The fracture energy is affected by the fracture mode of the composite specimens, i.e., the

interfacial fracture mode (I) results in smaller fracture energy, whereas the composite fracture (I-P) or (I-C) and concrete cohesion fracture mode (C) results in higher fracture energy.

- Applying the surface penetrant at the interface decreases the interfacial shear strength and results in the pure interfacial fracture mode (I), even if the surface roughness is high.
- The relationship of the load with opening and slip is linear up to the pre-peak region in all cases, but the post-peak behavior is hardly observed with the contact gauge technique due to brittle adhesion failure.
- The slip value is directly related to the opening value measured in the horizontal direction, i.e., an increase in the opening values results in a larger interfacial slip.

Acknowledgments

The author would like to acknowledge the scholarship grant provided by the Ministry of Education Culture, Sports, Science and Technology – Japan (MEXT) under the Top Global University project. The authors are also grateful to Dr. TAKAHASHI Jun and Mr. FUJIMA Seiji of Denka Co., Ltd. for providing valuable advice and materials (polymer cement mortar and silica fume) for this research. Besides, we are grateful to Mr. NISHINO Hideki of Fuji Chemical Co., Ltd. for providing the surface penetrant and guidance during the application process.

References

[1] Aravinthan, T. and Heldt, T. (2005). “Innovative strengthening technique using prestressed fiber wraps for bridge headstocks.” Proceedings of Australian Structural Engineering Conference, ISBN: 1877040371, 310-319.

[2] Tidarut, J., Zhang D. and Ueda, T. (2013). “Prediction of the post-peak behavior of reinforced concrete columns with and without FRP-jacketing.” Engineering Structures (Elsevier), 56:1511-1526.

[3] Alam, M. A., Ali, S. J., Zamin, M. J. and Kamal, N. M. (2014). “Effective method of repairing RC beam using externally bonded steel plate." Applied Mechanics and Materials, 567: 399-404.

[4] Zamin, J. and Alam, M. A. (2006). “Problems associated with plate bonding methods of strengthening reinforced concrete beams." Journal of Applied Sciences Research 2(10):703-708

[5] Alam, M. S., Kanakubo, T. and Yasojima, A. (2012). “Shear-Peeling Bond Strength between Continuous Fibre Sheet and Concrete." ACI Structural Journal, 75-82.

[6] Bruckner, A., Ortlepp, R. and Curbach, M. (2005). "Textile Reinforced Concrete for Strengthening in Bending and Shear." Materials and Structures, 38, 741-748.

[7] Wu, H. C. and Sun, P. (2005). "Fibre-reinforced cement-based composite sheets for structural retrofit." Proceedings of the International Symposium on Bond Behavior of FRP in Structures (BBFS).

[8] Chanh, T. M. T., Boonchai, S. and Ueda, T. (2014). "Investigation on the Bond Behavior Between PBO-FRCM Strengthening Material and Concrete." Journal of Advanced Concrete Technology, 12, 545-557.

[9] Zhang, D. (2009). “Research on PCM-Concrete Interface and PCM-Strengthened RC Beam.” Doctoral Thesis, Hokkaido University, Japan.

[10] Miura, S. (2017). “A Study on Interface Shear Behavior of PCM-Strengthened Concrete under High Temperature.” Master Thesis, Hokkaido University, Japan.

[11] Sakai, E. and Sugita, J. (1995). “Composite Mechanism of Polymer Modified Cement.” Cement

and Concrete Research, 25(1):127–135.

[12] Brien, J. V. and Mahboub, K. C. (2013). “Influence of polymer type on adhesion performance of blended cement mortar.” International Journal of Adhesion and Adhesives, 43: 7–13.

[13] Zhang, D., Ueda, T. and Furuuchi, H. (2011). "Intermediate Crack Debonding of Polymer Cement Mortar Overlay-Strengthened RC Beam." Journal of materials in civil engineering, 23(6): 857-865.

[14] Zhang, D., Ueda, T. and Furruchi, H. (2012). "Concrete cover separation failure of overlay strengthened reinforced concrete beams." Construction and Building Materials, 26: 735-745.

[15] Satoh, K. and Kodama, K. (2005). “Central Peeling Failure Behavior of Polymer Cement Mortar Retrofitting of Reinforced Concrete Beams.” Journal of Material in Civil Engineering, 17(2):126–136.

[16] Santos, P. M. D. and Júlio, E. B. S. (2010). “Recommended improvements to current shear friction provisions of model code.” Proceedings of the 3rd fib International Conference.

[17] Abu-tair A.I., Rigden S.R. and Burely E. (1996). “Testing the Bond between Repair Materials and Concrete Substrate.” ACI Materials Journal, 553-558.

[18] Santos, D. and Júlio S. (2013). “A state-of-the-art review of roughness quantification methods for concrete surfaces.” Construction and Building Materials, 38: 912–923.

[19] Austin S., Robins P. and Pan Y. (1995). “Tensile Bond Testing of Concrete Repairs.” Materials and Structures, 28: 249-59.

[20] Zhang D., Furuuchi H., Hori A., Fujima S. and Ueda T. (2008). “Influence of Interface Roughness on PCM-Concrete Interfacial Fracture Parameters.” Proceedings of 3rd ACF International Conference, HCM City, Vietnam, 15: 919-924.

[21] Das, K. (2012). “The effect of Silica Fume on the Properties of Concrete as Defined in Concrete Society Report 74, Cementitious Materials.” 37th Conference on Our World in Concrete and Structures, Singapore.

[22] Kurdowski, W. and Nocun-wczelik, W. (1983). “The tricalcium silicate hydration in the presence of active silica.” Cement and Concrete Research, 13(3), 341–348.

[23] Uchikawa, H. and Uchida, S. (1980). “Influence of pozzolans on the hydration of C3A.” 7th International Congress on the Chemistry of Cement, Paris, 23-29.

[24] Sugawara S., Koizumi T., Harada S. and Okazawa K. (2007). “Effect of reaction ratio of silica fume on strength development of 150N/mm^2 class concrete.” Concrete Research Technology, 18(95).

[25] Hayato, S., Mahmudul, H. M., Tamon, U., Katsuichi, M. and Jun, T. (2019). “A study on the effect of silica fume and surface penetrant on bonding strength for overlaying.” Journal of Asian Concrete Federation, 5(1):1-14.

[26] Kanezuka, T., Ito, M. and Katori, K. (2005). “Fresh state, strength, and structure system by changing the ratio of mixing silica fume.” Investigation by SOC Group.

[27] Fuji chemical Co. Ltd. (2009). “Guideline on the procedure of the application of silicate-based surface penetrant over the concrete surface.” Japan.

[28] Ueda, T., Khuram, R., Qian, Y. and Zhang, D. (2017). “Effects of Temperature and moisture on concrete-PCM interface performance.” Sustainable Civil Engineering Structures and Construction Materials, 171:71-79.

[29] Khuram, R., Zhang, D., Ueda, T. and Weiliang, J. (2016). “Investigation on concrete-PCM interface under elevated temperature: At material level and member level.” Construction and Building Materials, 125: 465–478.

[30] Zhang, D., Ueda, T. and Furuuchi, H. (2013). “Fracture mechanisms of polymer cement mortar: concrete interfaces.” Journal of Engineering Mechanics, 139:167-76.

[31] Ohama, Y. (1995). “Handbook of polymer-modified concrete and mortars-properties and process technology.” New Jersy, Noyes Publications.

[32] ASTM C39/39 M-05 (2013). “Standard Test Method for Compressive Strength of Cylindrical Concrete Specimens.” American Standard of Testing Materials.

[33] Momayez, A., Ramezanianpour, A., Rajaie, H. and Ehsani, M.R. (2004). “Bi-Surface Shear Test for Evaluating Bond between Existing and New Concrete.” ACI Materials Journal, 99-106.

[34] Santos, P. M. D. and Júlio, E. B. S. (2010). “Assessment of the Shear Strength between Concrete Layers.” 8th fib International Ph.D. Symposium in Civil Engineering, Denmark, 1-6.

[35] Tanaka, H., Yoshitake, I., Yamaguchi, Y. and Hamada, S. (2003). “A study of prototype of simple loading device giving pure shear force” Proceedings of the Japan Concrete Institute,

25(2):1003-1008.

[36] Rui, S., Júlio, E. B. S., Daniel, D.C and Santos, P. M. D. (2012). “Modified Slant Shear Test to Enforce Adhesive Failure.” Structural Faults and Repair, Edinburgh, Scotland.

[37] Alireza, V., Azadeh, J. J., Islam M. M. and Atorod A. (2020). “Experimental evaluation of concrete-to-UHPC bond strength with correlation to surface roughness for repair application.” Construction and Building Materials, 238: 1–11.

[38] Shuling, G., Xiaochong Z., Jinli, Q., Yadong, G. and Guanhua, H. (2019). “Study on the bonding properties of Engineered Cementitious Composites (ECC) and existing concrete exposed to high temperature.” Construction and Building Materials, 196: 330–344.

[39] Tian, J., Wu, X. and Zheng, Y. (2019). “Investigation of interface shear properties and mechanical model between ECC and concrete.” Construction and Building Materials, 223:12–27.

[40] Sahmaran, M., Yücel, H. E. and Yildirim, G. (2013). “Investigation of the bond between the concrete substrate and ECC overlays.” Journal of Materials in Civil Engineering, 26 (1): 167–174.

[41] Yu, J.T., Xu, W.L. and Zhang, Y.M. (2015). “Experiment study on fracture property of ECC-concrete interface.” Journal of Building Materials and Structures, 18(6): 958–963.

[42] Wang, B., Xu, S. and Liu, F. (2016). “Evaluation of tensile bonding strength between UHTCC repair materials and concrete substrate.” Construction and Building Materials, 112: 595–606.

[43] Rashid, K., Ueda, T., Zhang, D., Miyaguchi, K. and Nakai, H. (2015). “Experimental and analytical investigations on the behavior of the interface between concrete and polymer cement mortar under hygrothermal conditions.” Construction and Building Materials, 94: 414–425.